www.sciencemag.org/content/science.1246981/DC1

Supplementary Material for

Genetic Screens in Human Cells Using the CRISPR/Cas9 System

Tim Wang, Jenny J. Wei, David M. Sabatini,* Eric S. Lander*

*Corresponding author. E-mail: sabatini@wi.mit.edu (D.M.S.); lander@broadinstitute.org (E.S.L.)

Published 12 December 2013 on *Science* Express
DOI: 10.1126/science.1246981

This PDF file includes:

Other Supplementary Material for this manuscript includes the following:
(available at www.sciencemag.org/content/science.1246981/DC1)

Tables S1 to S4 and S8 as separate Excel files

Methods and Materials

Cell lines and vectors

Materials were obtained from the following sources: HL-60 were kindly provided by Robert Weinberg (Whitehead Institute, Cambridge, MA, USA); pCW57.1 Dox-inducible lentiviral vector, pX330-U6-Chimeric_BB-CBh-hSpCas9 vector, pLX304 lentiviral vector, and gRNA_AAVS1-T2 vector from Addgene.

Cell culture

Unless otherwise specified, 293T cells were cultured in DMEM (US Biological) and supplemented with 20% Inactivated Fetal Calf Serum (Sigma), 5 mM glutamine, and penicillin/streptomycin. HL60 and KBM7 cells were cultured in IMDM (Life Technologies) and supplemented with 20% IFS, 5 mM glutamine and penicillin/streptomycin.

Viability assay

Cells were seeded in 96-well tissue culture plates at 4000 cells/well in 200 µL of media under various treatment conditions. After 3 days, 35µL of CellTiter-Glo reagent (Promega) was added to each well, mixed for 5 minutes, and the luminescence was read on the SpectraMax M5 Luminometer (Molecular Devices). All experiments were performed in triplicate.

Dosing of screening agents

To determine the appropriate dose of 6-TG and etoposide for screening in KBM7 and HL60 cells, cells were seeded in 96-well tissue culture plates at 4000 cells/well in 200 µL of media and were treated in triplicate with varying concentrations of 6-TG and etoposide. A CellTiter-Glo cell viability assay was performed after 4 days to assess drug toxicity. Concentrations at which the viability of WT KBM7 and HL60 cells fell below 5% were chosen.

Vector construction

To construct the lentiviral doxycycline-inducible FLAG-Cas9 vector, the FLAG-Cas9 ORF from pX330-U6-Chimeric_BB-CBh-hSpCas9 was cloned into pCW57.1 between the AgeI and EcoRI sites. To construct the lentiviral sgRNA vector, the U6 promoter, the AAVS1-targeting sequence (GGGGCCACTAGGGACAGGAT), and the chimeric sgRNA scaffold from gRNA_AAVS1-T2 was cloned into pLX304 between the XhoI and NheI sites. Both plasmids are deposited in Addgene.

Genome-scale lentiviral sgRNA library design

All SpCas9 Protospacer Adjacent Motif (PAM) sites within 5 bases of a coding exon for all RefSeq transcript models were identified. If the first nucleotide of the protospacer/guide sequence did not begin with a ‘G’ (as is required for RNA polymerase III-dependent transcription), a ‘G’ was prepended. The sequences were then filtered for homopolymers spanning greater than 3 nucleotides. To avoid potential off-target cleavage, guide sequences that perfectly matched or had only 1 mismatch within the first 12 bases (the ‘non-seed’ region) with another genomic region were identified using the

short read aligner Bowtie and excluded (*33*). This specificity search was not performed for sgRNAs targeting ribosomal proteins. Subsequently, guide sequences that contained XbaI or NdeI sites were removed (although the library was eventually cloned via Gibson assembly) and guide sequences were filtered such that no two sgRNAs overlapped by more than 15 base pairs. After this step, all candidate sgRNAs for ribosomal protein genes were included in our final set. Additional candidate genes for screening were selected based upon their putative biological functions. Genes were excluded if they were not expressed (FPKM<1 in all tissues transcriptionally profiled in the Illumina Human Body Map and ENCODE project) or if 10 sgRNA sequences could not be designed. Finally for all remaining genes, 10 candidate sgRNAs were selected with a preference for sequences that (1) targeted constitutive exons, (2) were positioned closest downstream of the start codon and (3) had between 20% and 80% GC content. Sequences for non-targeting control sgRNAs were randomly generated and a specificity check, as described above, was performed. A second mini-library containing sgRNAs targeting ribosomal protein genes (2741 sgRNAs), *BCR* (228 sgRNAs), *ABL1* (223 sgRNAs) and 600 non-targeting control sgRNAs was designed as described above and used for negative selection screening and Cas9 immunoprecipitation/sgRNA sequencing in KBM7 cells.

Design of predicted genome-wide library

All SpCas9 Protospacer Adjacent Motif (PAM) sites within 6 bases of a coding exon for all CCDS transcript models were identified. If the first nucleotide of the protospacer/guide sequence did not begin with a 'G' (as is required for RNA polymerase III-dependent transcription), a 'G' was prepended. Sequences with %GC content between 40 to 80% that did not contain any homopolymers spanning greater than 4 nucleotides were considered. Because off-target matches may be unavoidable in some cases (eg. pseudogenes and duplicated genes), sequences were removed only if they mapped to more than 5 regions in the genome. Additionally for uniquely mapped sgRNAs, we then found the number off-target matches that differ from the guide sequence by only one base pair in the first twelve nucleotides (the 'non-seed' region). Olfactory receptor genes and genes with less than 5 sgRNA sequences fulfilling the criteria outlined above were excluded. For all remaining genes, 5-10 candidate sgRNAs were selected with a preference for sequences ordered by (1) the number of matches elsewhere in the genome (2) the number of 1-bp mismatched guide sequences that map elsewhere in the genome (3) the number of transcript models targeted for a given gene (4) the sgRNA score as predicted by the sgRNA efficacy algorithm and (5) the position along the transcript. Guide sequences were first filtered such that no two sgRNAs overlapped by more than 10 base pairs but this condition was relaxed to allow a 15 base pair overlap if no satisfactory sgRNAs could be found. Sequences for non-targeting control sgRNAs were randomly generated and a specificity check, as described above, was performed.

Genome-scale lentiviral sgRNA library construction

Oligonucleotides were synthesized on the CustomArray 12K and 90K arrays (CustomArray Inc.) and amplified as sub-pools in a nested PCR. A third round of PCR was performed to incorporate overhangs compatible for Gibson Assembly (NEB) into the lentiviral sgRNA AAVS1-targeting vector between the XbaI and NdeI sites. Gibson Assembly reaction products were transformed into chemically competent DH5alpha cells.

To preserve the diversity of the library, at least 20-fold coverage of each pool was recovered in each transformation and grown in liquid culture for 16-18 hours. Individual sub-pools of the genome-scale library are deposited in Addgene.

Virus production and transduction

Lentivirus was produced by the co-transfection of the lentiviral transfer vector with the Delta-VPR envelope and CMV VSV-G packaging plasmids into 293T cells using XTremeGene 9 transfection reagent (Roche). Media was changed 24 hours after transfection. The virus-containing supernatant was collected 48 and 72 hours after transfection and passed through a 0.45 μm filter to eliminate cells. Target cells in 6-well tissue culture plates were infected in media containing 8 μg/mL of polybrene and spin infection was performed by centrifugation at 2,200 rpm for 1 hour. 24 hours after infection, virus was removed and cells were selected with the appropriate antibiotics.

Cas9-KBM7 and Cas9-HL60 generation

Cas9-KBM7 and Cas9-HL60 cells were generated by lentiviral transduction of the dox-inducible FLAG-Cas9 vector. After 3 days of selection with puromycin, the cells were clonally sorted using an Aria II SORP (BD FACS) into 96-well tissue culture plates containing 200 μL of media. The level of FLAG-Cas9 expression in the presence and absence of 1μg/mL doxycycline was analyzed for several clonal populations by western blotting. Subsequently, a single colony with the greatest fold-change in Cas9 expression was selected from both cell lines for further studies.

Assessment of CRISPR/Cas9 cleavage efficiency

Cas9-KBM7 cells were infected with a sgRNA construct targeting the AASV1 locus at low MOI. At 0, 1, 2, 4, and 6 days post infection, cells were harvested for genomic DNA extraction. After amplification of the AAVS1 locus (primers sequences listed below), the SURVEYOR nuclease assay (Transgenomics) and gel quantification was performed as previous described (*14*). For deep sequencing of the target region, the AAVS1 locus was amplified with primers containing overhangs with adapters compatible with Illumina sequencing. Amplicons were sequenced on a MiSeq (Illumina) with a single-end 50 bp run. The resulting reads were aligned to the target reference sequence using the Smith-Waterman algorithm. Mutations were classified as a deletion, insertion, substitution or complex (a mixture of the previous 3 classes). Complex mutations were excluded in downstream analyses.

PCR primer sequences for Surveyor Assay
Primer 1: CCCCGTTCTCCTGTGGATTC
Primer 2: ATCCTCTCTGGCTCCATCGT

Primer sequences for MiSeq Sequencing Assay
Primer 1:
AATGATACGGCGACCACCGAGATCTACACCCCGTTCTCCTGTGGATTC
Primer 2: CAAGCAGAAGACGGCATACGAGATCATCCTCTCTGGCTCCATCGT
Illumina sequencing primer:
TCTGGTTCTGGGTACTTTTATCTGTCCCCTCCACCCCACAGT

Analysis of CRISPR/Cas9 specificity

Cas9-KBM7 cells were infected with a sgRNA construct targeting the AASV1 locus (sgAAVS1). Cells were selected for two weeks with blasticidin and harvested for genomic DNA extraction. Potential off-target cleavage sites were predicted by searching for genomic regions with sequence similarity to sgAAVS1 (no more than 3 mismatches were tolerated). Nested PCR primers were designed around these regions and the AAVS1 target region and used to amplify genomic DNA from sgAAVS1-modified and unmodified wild-type cells. PCR amplicons were sequenced on a MiSeq (Illumina) with a single-end 300 bp run. The resulting reads were filtered for the presence of matching forward and reverse primers and primer-dimer products were removed. Using the Needleman-Wunsch algorithm, amplicon reads were aligned to their respective reference sequences and assessed for the presence of an insertion or deletion.

Pooled screening

In all screens, 90 million target cells were transduced with viral sub-pools and selected with blasticidin 24 hours after infection for 3 days. For the 6-TG screen, Cas9-KBM7 cells were cultured in media containing 400 nM 6-TG. For screens with etoposide, Cas9-KBM7 and Cas9-HL60 cells were cultured in media containing 130 nM and 200 nM of etoposide, respectively. Cultures of untreated Cas9-KBM7 and Cas9-HL60 cells were also maintained in parallel. All cells were passaged every 3 days, and after 12 days, cells were harvested for genomic DNA extraction. In negative selection screens, 10 million cells were harvested for genomic DNA extraction 24 hours after infection. The remaining cells were maintained for 12 doublings before being harvested for genomic DNA extraction.

Pooled screening deconvolution and analysis

In both the positive and negative selection screens, sgRNA inserts were PCR amplified in a nested PCR and the resulting libraries were sequenced on a HiSeq 2500 (Illumina) with a single-end 50 bp run. The primer sequences for these reactions are provided below. Sequencing reads were aligned to the sgRNA library, and the abundance of each sgRNA was calculated. For the etoposide screens, the sgRNA abundances between the final treated and untreated populations were compared. To identify genes whose loss conferred resistance to etoposide, the (treated-untreated) $\log_2$ abundances of all sgRNAs targeting a gene was compared with the non-targeting sgRNAs using a one-sided Kolmogorov-Smirnov (K-S) test. p-values were corrected using the Benjamini-Hochberg method. To perform a sgRNA-level z-score analysis for all positive selection screens, the mean and standard deviation of the differential abundances of the non-targeting sgRNAs between treated versus untreated pools was determined. From these values, a z-score was calculated for all other sgRNAs.

In the negative selection screen, the $\log_2$ fold change in abundance of each sgRNA between the initial and final populations was computed. The significance of a gene hit was assessed by a two-sided K-S test between the $\log_2$ fold change of all sgRNAs targeting a gene and the values for all targeting sgRNAs. For ribosomal protein genes for which more sgRNAs were designed, random subsets of 10 sgRNAs were sampled for

significance testing and the p-value assigned to the gene was the median value after 50 random samplings. p-values were corrected using the Benjamini-Hochberg method. Gene-based scores were defined as the median $\log_2$ fold change of all sgRNAs targeting a given gene. For all genes, scores were calculated for both the HL60 and KBM7 screens. The two gene lists were sorted and the combined rank was determined. This metric was used for the Gene Set Enrichment Analysis of the C2 curated genes sets.

Primer sequences for sgRNA quantification
Outer primer 1: AGCGCTAGCTAATGCCAACTT
Outer primer 2: GCCGGCTCGAGTGTACAAAA
Inner primer 1:
AATGATACGGCGACCACCGAGATCTACACCGACTCGGTGCCACTTTT
Inner primer 2:
CAAGCAGAAGACGGCATACGAGATCnnnnnTTTCTTGGGTAGTTTGCAGTTTT
(nnnnn denotes the sample barcode)
Illumina sequencing primer:
CGGTGCCACTTTTTCAAGTTGATAACGGACTAGCCTTATTTTAACTTGCTATTT
CTAGCTCTAAAAC
Illumina indexing primer:
TTTCAAGTTACGGTAAGCATATGATAGTCCATTTTAAAACATAATTTTAAAAC
TGCAAACTACCCAAGAAA

Generation of sgRNA modified cell lines
Individual sgRNA constructs targeting CDK6 and TOP2A were cloned, lentivirus was produced, and target HL60 cells were transduced as described above. 24 hours after infection cells were cultured in doxycycline and blasticidin for 1 week before further experimentation.

Western blotting
Cells were lysed directly in Laemmeli sample buffer, separated on a NuPAGE Novex 8% Tris-Glycine gel, and transferred to a polyvinylidene difluoride membrane (Millipore). Immunoblots were processed according to standard procedures, using primary antibodies directed to S6K1 (CST), CDK6 (CST), FLAG (Sigma), and TOP2A (Topogen) and analyzed using enhanced chemiluminescence with HRP-conjugated anti-mouse and anti-rabbit secondary antibodies (Santa Cruz Biotechnology)**.**

FLAG-Cas9 immunoprecipitation and sgRNA-sequencing
10 million Cas9-KBM7 cells were transduced with lentivirus from the sgRNA mini-pool as described above. 24 hours after transduction, cells were rinsed once with ice-cold PBS and lysed in RIPA buffer (0.1% SDS, 1% sodium deoxycholate, 1% NP-40, 25 mM Tris-HCl pH 7.6, 150 mM NaCl, 1 mM EDTA, one tablet of EDTA-free protease inhibitor (per 25 ml) and 200U Murine RNAse Inhibitor (Sigma)). Cell lysate was homogenized using a 28-gauge syringe needle and incubated with rotation at 4°C for 15 minutes. The soluble fractions of cell lysates were isolated by centrifugation at 13,000 rpm in a refrigerated microcentrifuge for 10 min. The FLAG-M2 affinity gel (Sigma-Aldrich) was washed with lysis buffer three times, and 100 µl of a 50% slurry of the affinity gel was

then added to cleared cell lysates and incubated with rotation for 3 hours at 4°C. The beads were washed eight times with lysis buffer. Bound proteins were specifically eluted from the FLAG-M2 affinity gel with a competing FLAG peptide by incubation at room temperature for 10 minutes. The eluate was cleaned using a RNA Clean & Concentrator-5 column (Zymo Research), treated with TURBO DNase at 37°C for 10 minutes, and dephosphorylated with FastAP Thermosensitive Alkaline Phosphatase (Thermo Scientific) at 37°C for 10 minutes. The reaction was stopped by the addition of EDTA at a final concentration of 25 mM and heated at 68°C for 2 minutes after which the reaction was again cleaned using a RNA Clean & Concentrator-5 column. A sgRNA-specific reverse transcription reaction was performed using the primer listed below with SuperScript III (Life Technologies) at 54°C for 1 hour. The remainder of the library preparation protocol was performed as previously described except that a sgRNA-specific reverse primer was used for library amplification (*34*). In parallel, sgRNA barcode integrations in the DNA were also sequenced as described above. Sequencing reads from both libraries were aligned to the sgRNA library and the ratio of RNA reads to DNA reads for each sgRNA was used as a measure of Cas9 affinity.

Primer sequences for sgRNA-sequencing library preparation
sgRNA-specific reverse transcription primer: CTCGGTGCCACTTTTTCA
sgRNA-specific library amplification primer:
CAAGCAGAAGACGGCATACGAGATCTTCAAGTTGATAACGGACTAGCC

sgRNA efficacy analysis

Log_2 fold change (depletion) values for sgRNAs targeting ribosomal protein genes were used as a proxy for sgRNA efficacy. Depletion values were analyzed with respect to guide sequence GC content, the target exon position and the strand targeted. The predictive power of the features uncovered was examined by using a general linear model. sgRNAs against inessential ribosomal genes (*RPS4Y2*, *RPS4Y1*, *RPL22L1*, *RPL3L*, *RPL10L*, *RPL26L1*, *RPL39L*, *RPS27L*) were omitted from this analysis.

sgRNA efficacy prediction

A support-vector-machine classifier was used to predict sgRNA efficacy. The target sequences (each encoded by a vector of 80 binary variables representing the presence or absence of each nucleotide (A, C, T, G) at each position (1-20) along the target sequence) of ribosomal protein gene-targeting sgRNAs were used as inputs to the classifier which was trained on the change in abundance observed (encoded by a binary variable corresponding to 'weak' and 'strong' sgRNAs using a cutoff based on the bimodality of the distribution). Target sequences of sgRNAs targeting the 400 most essential non-ribosomal genes from the Cas9-KBM7 screens were used to predict efficacy. Class membership was again determined based on the bimodality of the distribution. sgRNAs against inessential ribosomal genes (*RPS4Y2*, *RPS4Y1*, *RPL22L1*, *RPL3L*, *RPL10L*, *RPL26L1*, *RPL39L*, *RPS27L*) were omitted from this analysis.

Supplementary Text

Note S1. Examination of potential sgRNA off-target sites.

We determine the expected number of potential off-target sites in the human genome and exome allowing for up to 3 mismatches in the non-seed region (first 12 base pairs) by the following calculation:

$$p_{20} = \left(\frac{1}{4}\right)^{20} = \text{ probability of a perfect 20 base pair match}$$

$$p_{PAM} = \left(\frac{1}{2}\right)\left(\frac{1}{4}\right) = \left(\frac{1}{8}\right) = \text{probability of a PAM sequence match (AG or GG allowed)}$$

$$MM_3 = \binom{12}{3}(4-1)^3 = \#\text{ of 3 base pair mismatch combinations in non-seed region}$$

$$MM_2 = \binom{12}{2}(4-1)^2 = \#\text{ of 2 base pair mismatch combinations in non-seed region}$$

$$MM_1 = \binom{12}{1}(4-1) = \#\text{ of 1 base pair mismatch combinations in non-seed region}$$

$$PM = 1 = \text{perfect match in non-seed region}$$

$$S_{genome} = 3 \times 10^9 = \text{ size of the human genome}$$

$$S_{exome} = 5 \times 10^7 = \text{ size of the human exome (UTR + CDS)}$$

$$OT_{Genome} = (p_{20})(p_{PAM})(MM_3 + MM_2 + MM_1 + PM)(S_{genome})$$
$$\approx 2.23 \text{ expected off-target sites in the genome per sgRNA}$$

$$OT_{Exome} = (p_{20})(p_{PAM})(MM_3 + MM_2 + MM_1 + PM)(S_{exome})$$
$$\approx 0.0372 \approx \frac{1}{27} \text{ expected off-target sites in the exome per sgRNA}$$

Fig. S1

A

Locus	Sequence	Genomic Coordinates	% Indel (mutant/total) sgAAVS1	WT
AAVS1	GGGGCCACTAGGGACAGGATTGG	chr19: 55627117-55627139	96.9% (7299/7531)	0% (0/440)
OT1	GGGGCTTCTAAGGACAGGATGGG	chr19: 16174987-16175009	29.5% (23724/80346)	0.07% (6/8088)
OT2	GGGGCAACTAGAGACAGGAAGGG	chr8: 22635581-22635603	2.46% (49/1990)	0% (0/961)
OT3	GGGGCCCCTGGGGACAGAATGGG	chr21: 42892942-42892964	1.36% (316/23230)	0.07% (2/2800)
OT4	GGGGCCAGTGGGGACAGGAAGGG	chr2: 232824540-232824562	0.68% (179/26249)	0.58% (20/3457)
OT5	GGTGCCACCAGGGAGAGGATGGG	chr22: 44699098-44699120	0.10% (1/1034)	0% (0/201)
OT6	GGTGCCACTAGGCACAGGAGCGG	chr8: 144885120-144885142	0.08% (2/2623)	0% (0/1247)
OT7	GGGGCCACTAGAGAAGGGATGGG	chr13: 37196607-37196629	0.03% (1/3998)	0% (0/662)
OT8	GGGGTCACTGGGGACAAGATTGG	chr15: 45827893-45827915	0.02% (2/11823)	0.05% (2/3750)
OT9	TGGGCCACTATGGACAGGAATGG	chr12: 108581676-108581698	0.01% (4/65617)	0.01% (1/8704)
OT10	GGGGCCACTAGGGAAAGAGTGGG	chr11: 47446589-47446611	0% (0/5340)	0.08% (1/1279)
OT11	GGGCCCACTAGGGTCAAGATAGG	chr2: 60390559-60390581	0% (0/555)	0% (0/153)
OT12	GGGGGAACTAGTGACAGGATAGG	chr20: 42338563-42338585	0% (0/4031)	0% (0/2153)
OT13	GGGGCCAGTAGGGGCAGGACAGG	chr20: 31034830-31034852	0% (0/249)	0% (0/326)

B

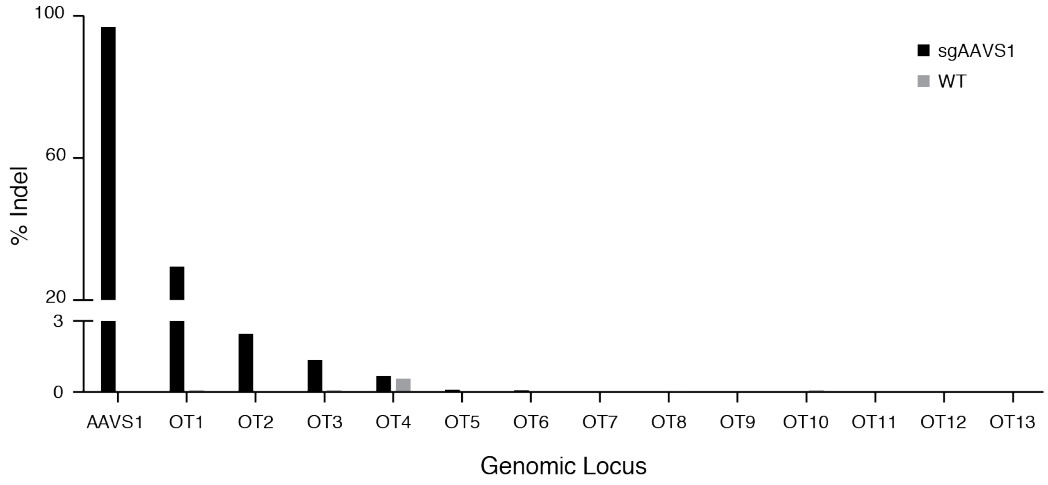

Fig. S1. Off-target cleavage analysis.

(A) AAVS1 and predicted sgAAVS1 off-target (OT) sites were individually amplified in a nested PCR from genomic DNA from sgAAVS1-modified and WT Cas9-KBM7 cells and analyzed by high-throughput sequencing. **(B)** Barplot summary of the results.

Fig. S2

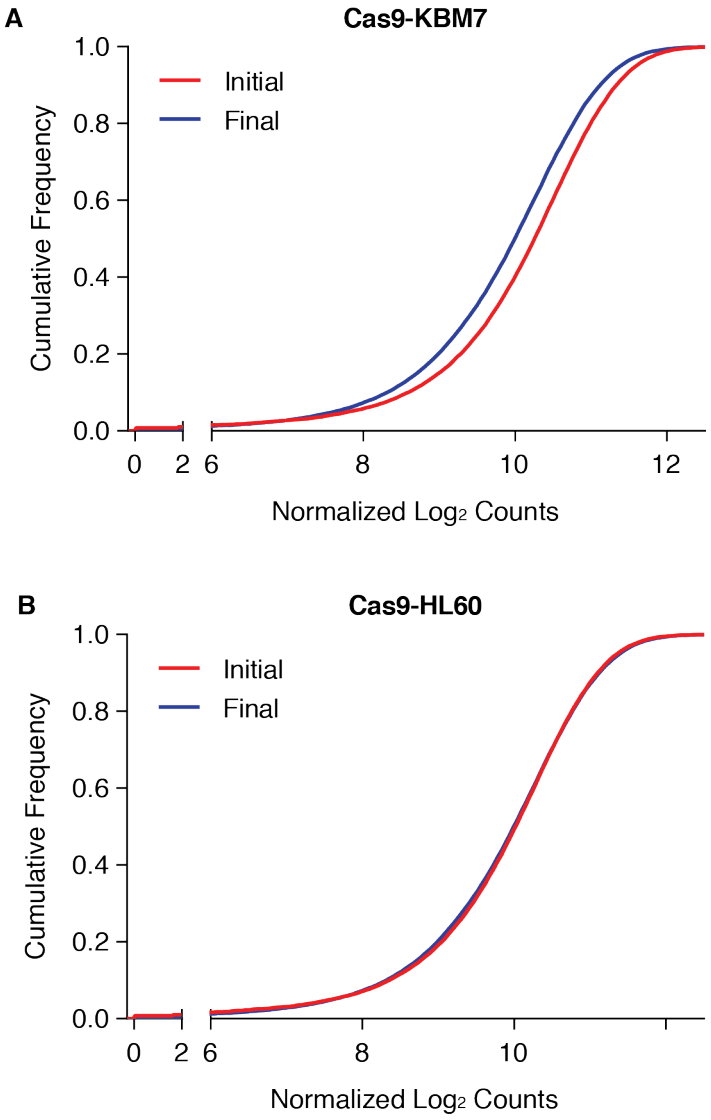

Fig. S2. Deep sequencing analysis of initial and final sgRNA library representation.

(A) Cumulative distribution function plots of sgRNA barcodes 24 hours after infection and after twelve cell doublings in Cas9-KBM7 and **(B)** Cas9-HL60 cells.

Fig. S3

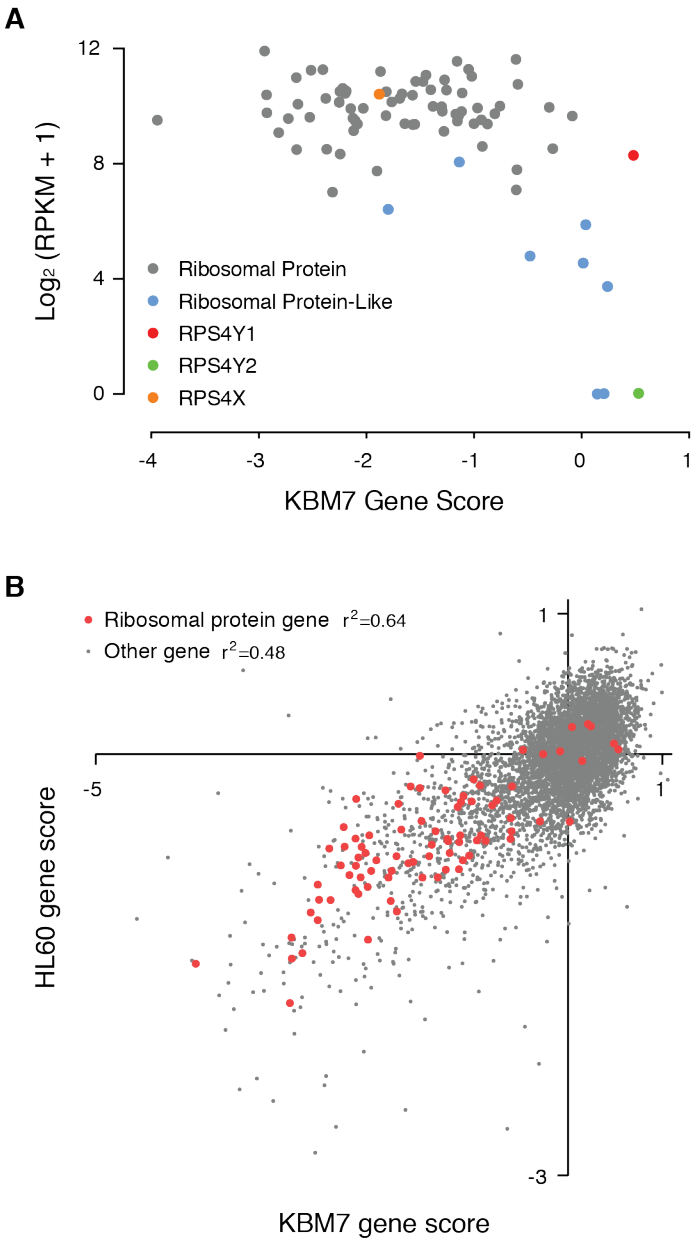

Fig. S3. Negative selection screens reveal essential genes.

(A) Ribosomal protein gene essentiality correlates with expression. Ribosomal protein gene depletion scores from the negative selection screen in Cas9-KBM7 cells are plotted against transcript abundance as determined by RNA-seq analysis of the KBM7 cell line. **(B)** Gene depletion scores of all genes screened are well correlated between Cas9-KBM7 and Cas9-HL60 cells.

Fig. S4

A

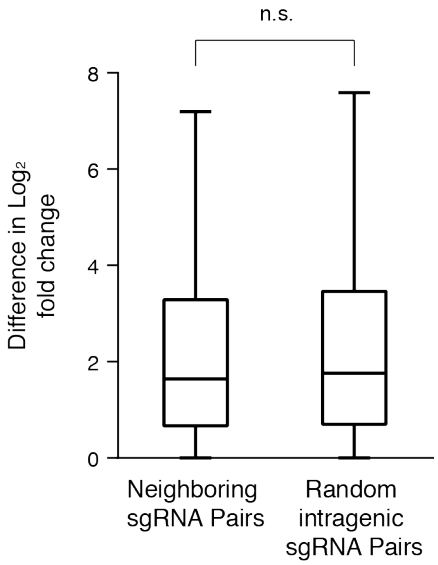

Fig. S4. High variability is observed between neighboring ribosomal protein gene-targeting sgRNAs.

(A) Differences in $\log_2$ fold change of neighboring sgRNA pairs are similar to differences in $\log_2$ fold change of random sgRNA pairs within the same gene indicating that local chromatin state does not significantly impact sgRNA efficacy.

Fig. S5

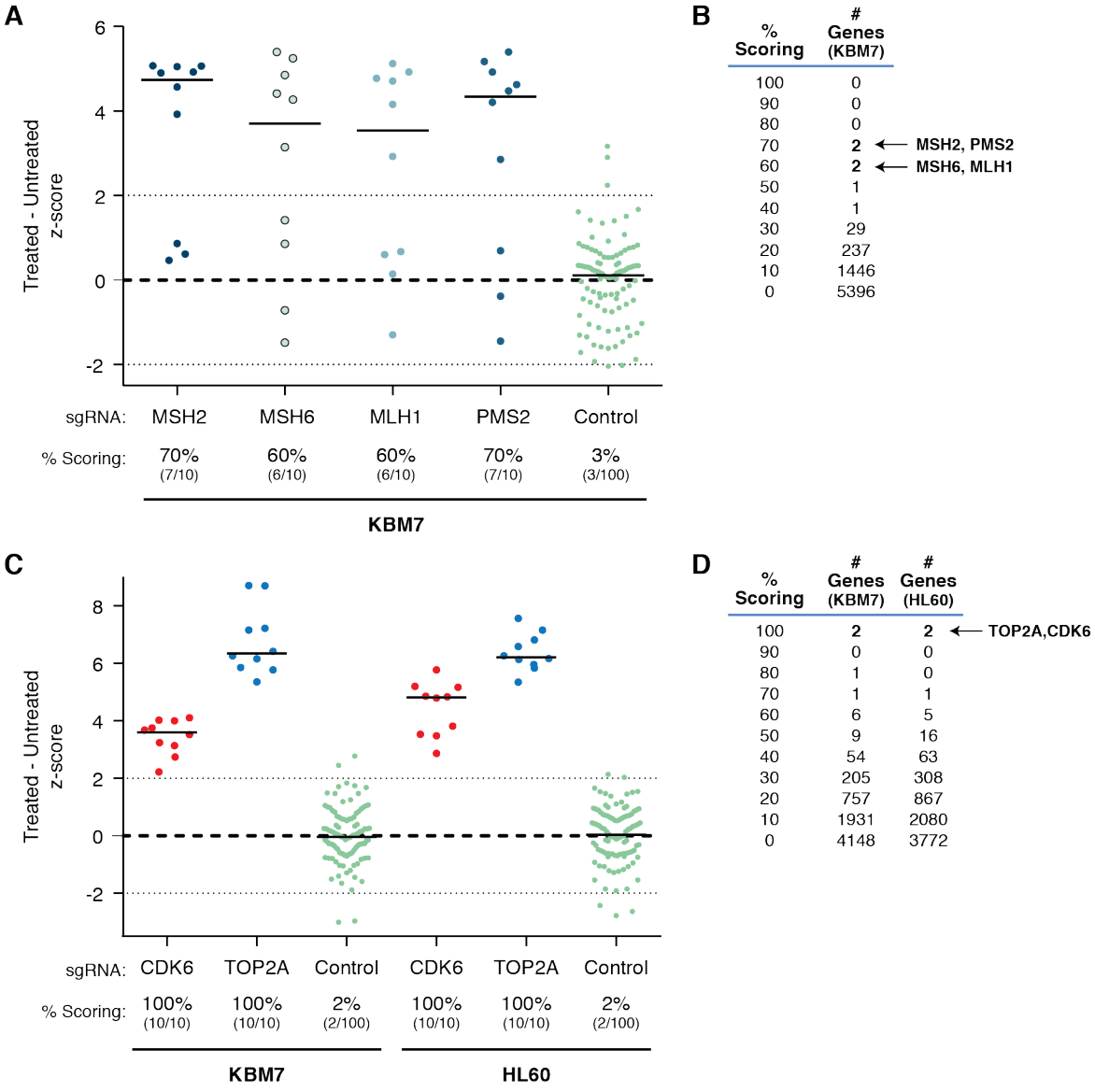

Fig. S5. z-score analysis of positive selection screens.

(A) z-scores of all sgRNAs targeting hit genes and non-targeting controls in the 6-TG screen. A sgRNA 'scores' if z>2. **(B)** Perfect discrimination between true and false positives is achieved at this significance threshold. **(C)** z-scores of all sgRNAs targeting hit genes and non-targeting controls in the etoposide screens. A sgRNA 'scores' if z>2. **(D)** Perfect discrimination between true and false positives is achieved at this significance threshold.

Table Captions

Table S1 (separate file)
Annotations for the genome-scale sgRNA library containing spacer sequences and target gene information.

Table S2 (separate file)
Gene-level data for etoposide screens in KBM7 and HL60 cells.

Table S3 (separate file)
Annotations for the mini sgRNA library containing spacer sequences and target gene information.

Table S4 (separate file)
Gene-level data for negative selection screens in KBM7 and HL60 cells.

Table S8 (separate file)
Annotations for the predicted genome-wide sgRNA library containing spacer sequences and target gene information.

Tables

Rank	Gene	Name	Yeast homolog	Essential in yeast?[a]	Evidence in other organisms
1	SF3B3	splicing factor 3b, subunit 3, 130kDa	RSE1	Yes	teg-4[b] CG13900[d]
2	RPP21	ribonuclease P/MRP 21kDa subunit	RPR2	Yes	
3	C1orf109	chromosome 1 open reading frame 109	-	-	c1orf109[f] human (*35*)
4	PCNA	proliferating cell nuclear antigen	POL30	Yes	pcn-1[b] mus209[e]
5	CDAN1	codanin 1	-	-	dlt[e] mouse (*36*)
6	PSMA7	proteasome (prosome, macropain) subunit, alpha type, 7	PRE6	Yes	pas-4[b]
7	GTF2B	general transcription factor IIB	SUA7	Yes	ttb-1[b]
8	ANAPC4	anaphase promoting complex subunit 4	APC4	Yes	emb-30[c]
9	CDC16	cell division cycle 16	CDC16	Yes	emb-27[b]
10	TPT1	tumor protein, translationally-controlled 1	TMA19	NO	tct-1[c] mouse (*37*)
11	SF3A3	splicing factor 3a, subunit 3, 60kDa	PRP9	Yes	T13H5.4[b] noi[e] sf3a3[f]
12	PREB	prolactin regulatory element binding	SEC12	Yes	sec-12[c]
13	HSPA9	heat shock 70kDa protein 9 (mortalin)	SSC1	Yes	hsp-6[b] Hsc70-5[e] Hspa9b[f]
14	POLR2A	polymerase (RNA) II (DNA directed) polypeptide A, 220kDa	RPO21	Yes	ama-1[b] RpII215[d]
15	PCF11	PCF11 cleavage and polyadenylation factor subunit	PCF11	Yes	pcf-11[b] CG10228[d]
16	POLR2L	polymerase (RNA) II (DNA directed) polypeptide L, 7.6kDa	RPB10	Yes	rpb-10[b] rpb10[d]
17	SPC24	SPC24, NDC80 kinetochore complex component	SPC24	Yes	

18	THAP1	THAP domain containing, apoptosis associated protein 1	-	-	human (*38*)
19	CDC123	cell division cycle 123	CDC123	Yes	
20	WDR74	WD repeat domain 74	NSA1	Yes	T06E6.1[b] CG7845[d]

Large-scale studies:
[a]S. cerevisiae (*1*)
[b]C. elegans (*39*)
[c]C. elegans (*40*)
[d]D. melanogaster (*41*)
[e]D. melanogaster (*42*)
[f]D. rerio (*43*)

Table S5. Independent evidence of essentiality for the top 20 non-ribosomal genes. Functional data from large-scale studies in model organisms and single gene studies in mice and human cell lines. 16 of 17 yeast homologs are essential. The sole except *TPT1* is essential in mice and C. elegans.

KEGG_DNA_REPLICATION				
Gene	Rank in Gene List	Raw Metric	Running ES	Core
RPA4	1045	5512	-0.12	No
POLD1	3054	3944	-0.378	No
POLE4	3938	3332	-0.474	No
MCM3	4717	2712.5	-0.556	No
RFC1	4959	2497.5	-0.561	No
LIG1	5098	2369	-0.551	No
POLD4	5587	1839.5	-0.592	Yes
POLE3	5640	1778	-0.57	Yes
RPA2	5668	1751.5	-0.544	Yes
POLA1	5689	1723.5	-0.518	Yes
RNASEH2B	6006	1322.5	-0.533	Yes
POLE	6039	1283	-0.509	Yes
RPA3	6180	1120	-0.499	Yes
RNASEH2C	6462	720.5	-0.51	Yes
DNA2	6496	673.5	-0.485	Yes
RFC4	6533	629.5	-0.461	Yes
MCM7	6542	615.5	-0.433	Yes
MCM2	6557	596	-0.405	Yes
RNASEH2A	6586	565.5	-0.38	Yes
RFC2	6668	465	-0.362	Yes
MCM5	6684	428.5	-0.335	Yes
MCM4	6724	385.5	-0.311	Yes
POLD3	6766	342	-0.287	Yes
POLD2	6806	286.5	-0.264	Yes
MCM6	6808	286	-0.234	Yes
PRIM1	6817	275	-0.206	Yes
PRIM2	6845	247.5	-0.18	Yes
RFC5	6867	218	-0.154	Yes
POLE2	6904	175.5	-0.13	Yes
RFC3	6917	153.5	-0.102	Yes
RPA1	6944	119	-0.076	Yes
FEN1	6972	72.5	-0.051	Yes
POLA2	6979	66.5	-0.022	Yes
PCNA	7026	13	1.00E-03	Yes
KEGG_RNA_POLYMERASE				
Gene	Rank in Gene List	Raw Metric	Running ES	Core

POLR1D	3555	3610	-0.466	No
POLR2F	3644	3534.5	-0.437	No
POLR3B	3902	3352.5	-0.432	No
POLR3GL	4839	2604.5	-0.524	No
POLR3A	5107	2363	-0.52	No
POLR3D	5251	2215	-0.499	No
POLR1A	5985	1354.5	-0.562	Yes
POLR3F	6247	1026.5	-0.557	Yes
POLR1C	6313	922.5	-0.525	Yes
POLR2H	6431	771	-0.5	Yes
ZNRD1	6694	412.5	-0.496	Yes
POLR3C	6709	398	-0.456	Yes
POLR2B	6744	368	-0.419	Yes
POLR2D	6763	348	-0.38	Yes
POLR2C	6776	335	-0.34	Yes
POLR1E	6791	312	-0.3	Yes
POLR1B	6844	249	-0.266	Yes
POLR2G	6919	152.5	-0.235	Yes
POLR3K	6948	108	-0.197	Yes
POLR3H	6983	63.5	-0.161	Yes
POLR2E	6998	47.5	-0.121	Yes
POLR2I	7007	37.5	-0.08	Yes
POLR2L	7014	27.5	-0.04	Yes
POLR2A	7018	24.5	0.002	Yes
KEGG_SPLICEOSOME				
Gene	Rank in Gene List	Raw Metric	Running ES	Core
HSPA1L	460	6160	-0.057	No
PRPF40B	1234	5313	-0.159	No
TCERG1	1450	5129	-0.18	No
HSPA6	2452	4350.5	-0.315	No
SRSF8	2672	4196.5	-0.337	No
HSPA2	3066	3934.5	-0.384	No
TRA2A	3276	3781.5	-0.404	No
SRSF4	3524	3624	-0.43	No
PQBP1	3603	3564	-0.432	No
U2SURP	3746	3466	-0.442	No
PPIL1	4504	2883.5	-0.542	No
DDX5	4508	2881	-0.533	No
WBP11	4689	2731.5	-0.549	No

SNRPB2	4710	2718	-0.542	No
DHX16	4751	2683	-0.538	No
DDX42	4956	2499	-0.558	No
SNRNP40	5269	2200	-0.593	No
DDX46	5457	1988.5	-0.61	Yes
PPIE	5472	1974.5	-0.603	Yes
PRPF31	5486	1958	-0.595	Yes
SRSF5	5499	1941.5	-0.587	Yes
LSM5	5615	1812	-0.594	Yes
U2AF1	5617	1810.5	-0.584	Yes
HNRNPA1	5676	1736	-0.583	Yes
USP39	5738	1674	-0.582	Yes
PRPF4	5788	1616.5	-0.579	Yes
DHX8	5893	1466.5	-0.585	Yes
LSM2	5958	1387	-0.584	Yes
AQR	5982	1355.5	-0.578	Yes
PLRG1	6062	1261	-0.58	Yes
U2AF2	6076	1250.5	-0.572	Yes
CCDC12	6110	1221	-0.567	Yes
THOC1	6112	1219	-0.557	Yes
DDX23	6147	1159	-0.552	Yes
CRNKL1	6183	1116	-0.548	Yes
LSM4	6186	1114.5	-0.538	Yes
ISY1	6204	1092	-0.531	Yes
RBMX	6210	1084.5	-0.522	Yes
CWC15	6252	1015	-0.518	Yes
SRSF9	6270	984.5	-0.511	Yes
RBM8A	6291	956	-0.504	Yes
SNRNP70	6321	915.5	-0.499	Yes
SNRNP27	6324	912.5	-0.489	Yes
SRSF10	6325	912	-0.48	Yes
SLU7	6337	894.5	-0.471	Yes
DHX38	6338	894	-0.462	Yes
SF3A1	6343	889	-0.453	Yes
XAB2	6371	856.5	-0.447	Yes
SNW1	6373	854	-0.437	Yes
SNRPD3	6395	829	-0.431	Yes
RBM17	6402	819.5	-0.422	Yes
CDC40	6406	814	-0.412	Yes

PRPF3	6442	746.5	-0.408	Yes
NHP2L1	6463	718	-0.401	Yes
THOC2	6469	709	-0.392	Yes
RBM25	6473	707.5	-0.383	Yes
HNRNPU	6478	698	-0.374	Yes
PRPF8	6486	685.5	-0.365	Yes
NAA38	6492	677.5	-0.356	Yes
SNRPA	6495	673.5	-0.346	Yes
SYF2	6514	654.5	-0.339	Yes
HNRNPM	6518	648.5	-0.33	Yes
BCAS2	6534	629	-0.323	Yes
EFTUD2	6569	578.5	-0.318	Yes
PRPF18	6605	544	-0.313	Yes
SMNDC1	6609	538.5	-0.304	Yes
PRPF38A	6641	499	-0.299	Yes
SF3B5	6643	494.5	-0.289	Yes
PRPF38B	6655	480.5	-0.281	Yes
SNRPB	6657	479.5	-0.271	Yes
ACIN1	6664	468.5	-0.262	Yes
DHX15	6686	426.5	-0.256	Yes
SNRPC	6727	383	-0.252	Yes
CTNNBL1	6739	375	-0.244	Yes
TRA2B	6741	373.5	-0.234	Yes
ZMAT2	6742	370	-0.224	Yes
SNRPD2	6771	339.5	-0.219	Yes
LSM7	6772	339.5	-0.209	Yes
PUF60	6783	325	-0.201	Yes
CDC5L	6801	297	-0.194	Yes
SART1	6805	291	-0.184	Yes
SRSF6	6807	286	-0.175	Yes
NCBP1	6826	264.5	-0.168	Yes
SNRPA1	6827	264.5	-0.158	Yes
SF3B2	6831	261	-0.149	Yes
SRSF7	6841	250.5	-0.14	Yes
DDX39B	6852	241	-0.132	Yes
RBM22	6859	230.5	-0.123	Yes
PRPF19	6864	224.5	-0.114	Yes
HNRNPK	6894	189	-0.108	Yes
SF3A2	6912	167.5	-0.101	Yes

BUD31	6923	149.5	-0.093	Yes
PRPF6	6927	147	-0.084	Yes
PCBP1	6928	142.5	-0.074	Yes
EIF4A3	6939	129	-0.066	Yes
NCBP2	6942	121.5	-0.056	Yes
SNRNP200	6951	101.5	-0.048	Yes
TXNL4A	6963	88.5	-0.04	Yes
SRSF3	6975	69.5	-0.031	Yes
SRSF2	6989	54.5	-0.024	Yes
SRSF1	7002	44	-0.016	Yes
SF3A3	7020	23.5	-0.008	Yes
SF3B3	7030	8	0.00E+00	Yes
BIOCARTA_PROTEASOME_PATHWAY				
Gene	Rank in Gene List	Raw Metric	Running ES	Core
UBE2A	319	6328.5	-0.007	No
UBE3A	2034	4674.5	-0.213	No
PSMD8	2876	4054.5	-0.295	No
PSMA4	5599	1831	-0.645	Yes
PSMC4	5706	1708.5	-0.622	Yes
PSMB6	5800	1603	-0.596	Yes
PSMD12	6056	1267	-0.594	Yes
PSMA3	6094	1233	-0.561	Yes
RPN2	6161	1148	-0.532	Yes
PSMB4	6202	1096	-0.499	Yes
PSMD14	6366	862	-0.484	Yes
PSMB3	6394	829	-0.45	Yes
PSMC2	6438	753	-0.417	Yes
PSMB1	6516	652.5	-0.39	Yes
PSMB5	6649	487.5	-0.37	Yes
PSMA2	6674	451.5	-0.335	Yes
PSMA1	6716	392.5	-0.303	Yes
PSMB2	6762	348	-0.271	Yes
PSMA5	6768	341.5	-0.233	Yes
PSMD6	6795	306.5	-0.198	Yes
PSMB7	6813	281.5	-0.162	Yes
PSMC6	6834	258	-0.126	Yes
PSMA6	6855	238	-0.091	Yes
PSMC3	6916	155	-0.061	Yes
PSMD11	6934	133.5	-0.025	Yes

PSMA7	7027	13	0.00E+00	Yes

Table S6 Gene Set Enrichment Analysis
Gene composition and scores of the enriched gene sets highlighted in Fig. 3D.

Variable	Degrees of Freedom	Variance Explained (r^2)
Full Sequence (combined)	2460	1
First 4 nucleotides (combined)	250	0.17
Middle 4 nucleotides (combined)	251	0.133
Last 4 nucleotides (combined)	251	0.291
First 4 nucleotides (additive)	12	0.04
Middle 4 nucleotides (additive)	12	0.02
Last 4 nucleotides (additive)	12	0.129
GC Content	14	0.025
gRNA Strand	1	0.014
Exon Type	2	0.013

Table S7 Analysis of features influencing sgRNA efficacy
Summary of the variance in ribosomal protein-targeting sgRNA $\log_2$ fold changes explained by various features of sgRNAs using a general linear model.

References and Notes

1. G. Giaever, A. M. Chu, L. Ni, C. Connelly, L. Riles, S. Véronneau, S. Dow, A. Lucau-Danila, K. Anderson, B. André, A. P. Arkin, A. Astromoff, M. El-Bakkoury, R. Bangham, R. Benito, S. Brachat, S. Campanaro, M. Curtiss, K. Davis, A. Deutschbauer, K. D. Entian, P. Flaherty, F. Foury, D. J. Garfinkel, M. Gerstein, D. Gotte, U. Güldener, J. H. Hegemann, S. Hempel, Z. Herman, D. F. Jaramillo, D. E. Kelly, S. L. Kelly, P. Kötter, D. LaBonte, D. C. Lamb, N. Lan, H. Liang, H. Liao, L. Liu, C. Luo, M. Lussier, R. Mao, P. Menard, S. L. Ooi, J. L. Revuelta, C. J. Roberts, M. Rose, P. Ross-Macdonald, B. Scherens, G. Schimmack, B. Shafer, D. D. Shoemaker, S. Sookhai-Mahadeo, R. K. Storms, J. N. Strathern, G. Valle, M. Voet, G. Volckaert, C. Y. Wang, T. R. Ward, J. Wilhelmy, E. A. Winzeler, Y. Yang, G. Yen, E. Youngman, K. Yu, H. Bussey, J. D. Boeke, M. Snyder, P. Philippsen, R. W. Davis, M. Johnston, Functional profiling of the Saccharomyces cerevisiae genome. *Nature* **418**, 387–391 (2002). doi:10.1038/nature00935 Medline

2. M. Costanzo, A. Baryshnikova, J. Bellay, Y. Kim, E. D. Spear, C. S. Sevier, H. Ding, J. L. Koh, K. Toufighi, S. Mostafavi, J. Prinz, R. P. St Onge, B. VanderSluis, T. Makhnevych, F. J. Vizeacoumar, S. Alizadeh, S. Bahr, R. L. Brost, Y. Chen, M. Cokol, R. Deshpande, Z. Li, Z. Y. Lin, W. Liang, M. Marback, J. Paw, B. J. San Luis, E. Shuteriqi, A. H. Tong, N. van Dyk, I. M. Wallace, J. A. Whitney, M. T. Weirauch, G. Zhong, H. Zhu, W. A. Houry, M. Brudno, S. Ragibizadeh, B. Papp, C. Pál, F. P. Roth, G. Giaever, C. Nislow, O. G. Troyanskaya, H. Bussey, G. D. Bader, A. C. Gingras, Q. D. Morris, P. M. Kim, C. A. Kaiser, C. L. Myers, B. J. Andrews, C. Boone, The genetic landscape of a cell. *Science* **327**, 425–431 (2010). doi:10.1126/science.1180823

3. J. E. Carette, C. P. Guimaraes, M. Varadarajan, A. S. Park, I. Wuethrich, A. Godarova, M. Kotecki, B. H. Cochran, E. Spooner, H. L. Ploegh, T. R. Brummelkamp, Haploid genetic screens in human cells identify host factors used by pathogens. *Science* **326**, 1231–1235 (2009). doi:10.1126/science.1178955

4. G. Guo, W. Wang, A. Bradley, Mismatch repair genes identified using genetic screens in Blm-deficient embryonic stem cells. *Nature* **429**, 891–895 (2004). doi:10.1038/nature02653 Medline

5. A. Fire, S. Xu, M. K. Montgomery, S. A. Kostas, S. E. Driver, C. C. Mello, Potent and specific genetic interference by double-stranded RNA in *Caenorhabditis elegans*. *Nature* **391**, 806–811 (1998). doi:10.1038/35888 Medline

6. T. R. Brummelkamp, R. Bernards, R. Agami, A system for stable expression of short interfering RNAs in mammalian cells. *Science* **296**, 550–553 (2002). doi:10.1126/science.1068999

7. J. Moffat, D. A. Grueneberg, X. Yang, S. Y. Kim, A. M. Kloepfer, G. Hinkle, B. Piqani, T. M. Eisenhaure, B. Luo, J. K. Grenier, A. E. Carpenter, S. Y. Foo, S. A. Stewart, B. R. Stockwell, N. Hacohen, W. C. Hahn, E. S. Lander, D. M. Sabatini, D. E. Root, A lentiviral RNAi library for human and mouse genes applied to an arrayed viral high-content screen. *Cell* **124**, 1283–1298 (2006). doi:10.1016/j.cell.2006.01.040 Medline

8. V. N. Ngo, R. E. Davis, L. Lamy, X. Yu, H. Zhao, G. Lenz, L. T. Lam, S. Dave, L. Yang, J. Powell, L. M. Staudt, A loss-of-function RNA interference screen for molecular targets in cancer. *Nature* **441**, 106–110 (2006). doi:10.1038/nature04687 Medline

9. H. W. Cheung, G. S. Cowley, B. A. Weir, J. S. Boehm, S. Rusin, J. A. Scott, A. East, L. D. Ali, P. H. Lizotte, T. C. Wong, G. Jiang, J. Hsiao, C. H. Mermel, G. Getz, J. Barretina, S. Gopal, P. Tamayo, J. Gould, A. Tsherniak, N. Stransky, B. Luo, Y. Ren, R. Drapkin, S. N. Bhatia, J. P. Mesirov, L. A. Garraway, M. Meyerson, E. S. Lander, D. E. Root, W. C. Hahn, Systematic investigation of genetic vulnerabilities across cancer cell lines reveals lineage-specific dependencies in ovarian cancer. *Proc. Natl. Acad. Sci. U.S.A.* **108**, 12372–12377 (2011). doi:10.1073/pnas.1109363108 Medline

10. C. J. Echeverri, P. A. Beachy, B. Baum, M. Boutros, F. Buchholz, S. K. Chanda, J. Downward, J. Ellenberg, A. G. Fraser, N. Hacohen, W. C. Hahn, A. L. Jackson, A. Kiger, P. S. Linsley, L. Lum, Y. Ma, B. Mathey-Prévôt, D. E. Root, D. M. Sabatini, J. Taipale, N. Perrimon, R. Bernards, Minimizing the risk of reporting false positives in large-scale RNAi screens. *Nat. Methods* **3**, 777–779 (2006). doi:10.1038/nmeth1006-777 Medline

11. M. Booker, A. A. Samsonova, Y. Kwon, I. Flockhart, S. E. Mohr, N. Perrimon, False negative rates in Drosophila cell-based RNAi screens: A case study. *BMC Genomics* **12**, 50 (2011). doi:10.1186/1471-2164-12-50 Medline

12. W. G. Kaelin Jr., Use and abuse of RNAi to study mammalian gene function. *Science* **337**, 421–422 (2012). doi:10.1126/science.1225787

13. R. Barrangou, C. Fremaux, H. Deveau, M. Richards, P. Boyaval, S. Moineau, D. A. Romero, P. Horvath, CRISPR provides acquired resistance against viruses in prokaryotes. *Science* **315**, 1709–1712 (2007). doi:10.1126/science.1138140

14. L. Cong, F. A. Ran, D. Cox, S. Lin, R. Barretto, N. Habib, P. D. Hsu, X. Wu, W. Jiang, L. A. Marraffini, F. Zhang, Multiplex genome engineering using CRISPR/Cas systems. *Science* **339**, 819–823 (2013). doi:10.1126/science.1231143

15. P. Mali, L. Yang, K. M. Esvelt, J. Aach, M. Guell, J. E. DiCarlo, J. E. Norville, G. M. Church, RNA-guided human genome engineering via Cas9. *Science* **339**, 823–826 (2013). doi:10.1126/science.1232033

16. W. Y. Hwang, Y. Fu, D. Reyon, M. L. Maeder, S. Q. Tsai, J. D. Sander, R. T. Peterson, J. R. Yeh, J. K. Joung, Efficient genome editing in zebrafish using a CRISPR-Cas system. *Nat. Biotechnol.* **31**, 227–229 (2013). doi:10.1038/nbt.2501 Medline

17. M. Jinek, K. Chylinski, I. Fonfara, M. Hauer, J. A. Doudna, E. Charpentier, A programmable dual-RNA-guided DNA endonuclease in adaptive bacterial immunity. *Science* **337**, 816–821 (2012). doi:10.1126/science.1225829

18. T. Horii, D. Tamura, S. Morita, M. Kimura, I. Hatada, Generation of an ICF syndrome model by efficient genome editing of human induced pluripotent stem cells using the CRISPR system. *Int. J. Mol. Sci.* **14**, 19774–19781 (2013). doi:10.3390/ijms141019774 Medline

19. H. Wang, H. Yang, C. S. Shivalila, M. M. Dawlaty, A. W. Cheng, F. Zhang, R. Jaenisch, One-step generation of mice carrying mutations in multiple genes by CRISPR/Cas-mediated genome engineering. *Cell* **153**, 910–918 (2013). doi:10.1016/j.cell.2013.04.025 Medline

20. P. D. Hsu, D. A. Scott, J. A. Weinstein, F. A. Ran, S. Konermann, V. Agarwala, Y. Li, E. J. Fine, X. Wu, O. Shalem, T. J. Cradick, L. A. Marraffini, G. Bao, F. Zhang, DNA targeting specificity of RNA-guided Cas9 nucleases. *Nat. Biotechnol.* **31**, 827–832 (2013). doi:10.1038/nbt.2647 Medline

21. Y. Fu, J. A. Foden, C. Khayter, M. L. Maeder, D. Reyon, J. K. Joung, J. D. Sander, High-frequency off-target mutagenesis induced by CRISPR-Cas nucleases in human cells. *Nat. Biotechnol.* **31**, 822–826 (2013). doi:10.1038/nbt.2623 Medline

22. V. Pattanayak, S. Lin, J. P. Guilinger, E. Ma, J. A. Doudna, D. R. Liu, High-throughput profiling of off-target DNA cleavage reveals RNA-programmed Cas9 nuclease specificity. *Nat. Biotechnol.* **31**, 839–843 (2013). doi:10.1038/nbt.2673 Medline

23. T. Yan, S. E. Berry, A. B. Desai, T. J. Kinsella, DNA mismatch repair (MMR) mediates 6-thioguanine genotoxicity by introducing single-strand breaks to signal a G2-M arrest in MMR-proficient RKO cells. *Clin. Cancer Res.* **9**, 2327–2334 (2003). Medline

24. R. D. Kolodner, G. T. Marsischky, Eukaryotic DNA mismatch repair. *Curr. Opin. Genet. Dev.* **9**, 89–96 (1999). doi:10.1016/S0959-437X(99)80013-6 Medline

25. D. J. Burgess, J. Doles, L. Zender, W. Xue, B. Ma, W. R. McCombie, G. J. Hannon, S. W. Lowe, M. T. Hemann, Topoisomerase levels determine chemotherapy response in vitro and in vivo. *Proc. Natl. Acad. Sci. U.S.A.* **105**, 9053–9058 (2008). doi:10.1073/pnas.0803513105 Medline

26. B. Scappini, S. Gatto, F. Onida, C. Ricci, V. Divoky, W. G. Wierda, M. Andreeff, L. Dong, K. Hayes, S. Verstovsek, H. M. Kantarjian, M. Beran, Changes associated with the development of resistance to imatinib (STI571) in two leukemia cell lines expressing p210 Bcr/Abl protein. *Cancer* **100**, 1459–1471 (2004). doi:10.1002/cncr.20131 Medline

27. S. Xue, M. Barna, Specialized ribosomes: A new frontier in gene regulation and organismal biology. *Nat. Rev. Mol. Cell Biol.* **13**, 355–369 (2012). doi:10.1038/nrm3359 Medline

28. C. M. Johnston, F. L. Lovell, D. A. Leongamornlert, B. E. Stranger, E. T. Dermitzakis, M. T. Ross, Large-scale population study of human cell lines indicates that dosage compensation is virtually complete. *PLOS Genet.* **4**, e9 (2008). doi:10.1371/journal.pgen.0040009 Medline

29. A. Subramanian, P. Tamayo, V. K. Mootha, S. Mukherjee, B. L. Ebert, M. A. Gillette, A. Paulovich, S. L. Pomeroy, T. R. Golub, E. S. Lander, J. P. Mesirov, Gene set enrichment analysis: a knowledge-based approach for interpreting genome-wide expression profiles. *Proc. Natl. Acad. Sci. U.S.A.* **102**, 15545–15550 (2005). doi:10.1073/pnas.0506580102 Medline

30. F. A. Ran, P. D. Hsu, C. Y. Lin, J. S. Gootenberg, S. Konermann, A. E. Trevino, D. A. Scott, A. Inoue, S. Matoba, Y. Zhang, F. Zhang, Double nicking by RNA-guided CRISPR Cas9 for enhanced genome editing specificity. *Cell* **154**, 1380–1389 (2013). doi:10.1016/j.cell.2013.08.021 Medline

31. P. Mali, J. Aach, P. B. Stranges, K. M. Esvelt, M. Moosburner, S. Kosuri, L. Yang, G. M. Church, CAS9 transcriptional activators for target specificity screening and paired nickases for cooperative genome engineering. *Nat. Biotechnol.* **31**, 833–838 (2013). doi:10.1038/nbt.2675 Medline

32. K. Yoshimoto, M. Mizoguchi, N. Hata, H. Murata, R. Hatae, T. Amano, A. Nakamizo, T. Sasaki, Complex DNA repair pathways as possible therapeutic targets to overcome temozolomide resistance in glioblastoma. *Front. Oncol.* **2**, 186 (2012). doi:10.3389/fonc.2012.00186 Medline

33. B. Langmead, S. L. Salzberg, Fast gapped-read alignment with Bowtie 2. *Nat. Methods* **9**, 357–359 (2012). doi:10.1038/nmeth.1923 Medline

34. J. M. Engreitz, A. Pandya-Jones, P. McDonel, A. Shishkin, K. Sirokman, C. Surka, S. Kadri, J. Xing, A. Goren, E. S. Lander, K. Plath, M. Guttman, The Xist lncRNA exploits three-dimensional genome architecture to spread across the X chromosome. *Science* **341**, 1237973 (2013). doi:10.1126/science.1237973

35. S. S. Liu, H. X. Zheng, H. D. Jiang, J. He, Y. Yu, Y. P. Qu, L. Yue, Y. Zhang, Y. Li, Identification and characterization of a novel gene, c1orf109, encoding a CK2 substrate that is involved in cancer cell proliferation. *J. Biomed. Sci.* **19**, 49 (2012). doi:10.1186/1423-0127-19-49 Medline

36. R. Renella, N. A. Roberts, J. M. Brown, M. De Gobbi, L. E. Bird, T. Hassanali, J. A. Sharpe, J. Sloane-Stanley, D. J. Ferguson, J. Cordell, V. J. Buckle, D. R. Higgs, W. G. Wood, Codanin-1 mutations in congenital dyserythropoietic anemia type 1 affect HP1α localization in erythroblasts. *Blood* **117**, 6928–6938 (2011). doi:10.1182/blood-2010-09-308478 Medline

37. S. H. Chen, P. S. Wu, C. H. Chou, Y. T. Yan, H. Liu, S. Y. Weng, H. F. Yang-Yen, A knockout mouse approach reveals that TCTP functions as an essential factor for cell proliferation and survival in a tissue- or cell type-specific manner. *Mol. Biol. Cell* **18**, 2525–2532 (2007). doi:10.1091/mbc.E07-02-0188 Medline

38. C. Cayrol, C. Lacroix, C. Mathe, V. Ecochard, M. Ceribelli, E. Loreau, V. Lazar, P. Dessen, R. Mantovani, L. Aguilar, J. P. Girard, The THAP-zinc finger protein THAP1 regulates endothelial cell proliferation through modulation of pRB/E2F cell-cycle target genes. *Blood* **109**, 584–594 (2007). doi:10.1182/blood-2006-03-012013 Medline

39. B. Sönnichsen, L. B. Koski, A. Walsh, P. Marschall, B. Neumann, M. Brehm, A. M. Alleaume, J. Artelt, P. Bettencourt, E. Cassin, M. Hewitson, C. Holz, M. Khan, S. Lazik, C. Martin, B. Nitzsche, M. Ruer, J. Stamford, M. Winzi, R. Heinkel, M. Röder, J. Finell, H. Häntsch, S. J. Jones, M. Jones, F. Piano, K. C. Gunsalus, K. Oegema, P. Gönczy, A. Coulson, A. A. Hyman, C. J. Echeverri, Full-genome RNAi profiling of early embryogenesis in *Caenorhabditis elegans*. *Nature* **434**, 462–469 (2005). doi:10.1038/nature03353 Medline

40. J.-F. Rual, J. Ceron, J. Koreth, T. Hao, A. S. Nicot, T. Hirozane-Kishikawa, J. Vandenhaute, S. H. Orkin, D. E. Hill, S. van den Heuvel, M. Vidal, Toward improving Caenorhabditis elegans phenome mapping with an ORFeome-based RNAi library. *Genome Res.* **14**, (10B), 2162–2168 (2004). doi:10.1101/gr.2505604 Medline

41. J. L. Mummery-Widmer, M. Yamazaki, T. Stoeger, M. Novatchkova, S. Bhalerao, D. Chen, G. Dietzl, B. J. Dickson, J. A. Knoblich, Genome-wide analysis of Notch signalling in *Drosophila* by transgenic RNAi. *Nature* **458**, 987–992 (2009). doi:10.1038/nature07936 Medline

42. A. C. Spradling, D. Stern, A. Beaton, E. J. Rhem, T. Laverty, N. Mozden, S. Misra, G. M. Rubin, The Berkeley Drosophila Genome Project gene disruption project: Single P-element insertions mutating 25% of vital *Drosophila* genes. *Genetics* **153**, 135–177 (1999). Medline

43. A. Amsterdam, R. M. Nissen, Z. Sun, E. C. Swindell, S. Farrington, N. Hopkins, Identification of 315 genes essential for early zebrafish development. *Proc. Natl. Acad. Sci. U.S.A.* **101**, 12792–12797 (2004). doi:10.1073/pnas.0403929101 Medline